INTERNATIONAL JOURNAL OF CLIMATOLOGY
Int. J. Climatol. (2015)
Published online in Wiley Online Library
(wileyonlinelibrary.com) DOI: 10.1002/joc.4383

RMetS
Royal Meteorological Society

An analysis of teleconnections in the Mediterranean region using RegCM4

James M. Ciarlo`* and Noel J. Aquilina
Department of Physics, University of Malta, Msida, Malta

ABSTRACT: Atmospheric teleconnections have an important influence on the variability of the Mediterranean climate. This region has a unique and sensitive climate due to its complex topography and atmospheric circulation, thus making it challenging in climate simulations. This article focuses on the representation of five teleconnections in and around the Mediterranean region and how they affect one another and the region.

The Regional Climate Model, RegCM4, has been used to simulate the climate from 1969 to 1999 for a domain covering the Mediterranean and the surrounding region. A generalized method for calculating the indices for these patterns was identified and the corresponding indices were constructed from the modelled data and compared with reanalysis data. The modelled data was found to be highly correlated with the 20th Century Reanalysis data and the probability density functions (PDFs) were very similar to the reanalysis data, showing that the teleconnections were successfully represented within the model.

Maps of the influence of these teleconnections on temperature, precipitation and wind were also comparable to the reanalysis data, thereby suggesting that model data can be used for future projections of teleconnections and their effects on these parameters. With the use of this high-resolution data, inter-pattern relationships suggested in previous studies (such as that between the Mediterranean Oscillation and North sea-Caspian Pattern) became more evident. This article also shows how the influence of teleconnections on winds affects the circulation and hence the temperature and precipitation of the region.

KEY WORDS teleconnections; interactions; Mediterranean; Regional Climate Model; RegCM4

Received 27 October 2014; Revised 27 March 2015; Accepted 22 April 2015

1. Introduction

The climate in the North Atlantic and European region is strongly affected by the Icelandic Low and Azores High pressure systems. Their influence extends all over the Northern Hemisphere especially over the Mediterranean Sea. This inland sea is composed of complex characteristics that give it a unique climate and a higher sensitivity to climate change (Lionello *et al.*, 2006; Martin-Vide and Lopez-Bustins, 2006) and thus more challenging for climate modelling. Apart from its complex orography the climate in this region is also affected by atmospheric circulation patterns. Typically, coupled semi-permanent pressure systems such as the Azores High and the Icelandic Low (Bauer and Morikawa, 1976; Christoforou and Hameed, 1997; McIlveen, 2010; Ackerman and Knox, 2011) give rise to circulation patterns (Hurrell *et al.*, 2003), commonly referred to as teleconnections (Meehl and van Loon, 1979; Wallace and Gutzler, 1981; Esbensen, 1984; Barnston and Livezey, 1987; Rogers, 1990; Kutiel and Benaroch, 2002; Kutiel *et al.*, 2002; Hurrell *et al.*, 2003; Kutiel and Helfman, 2004; Krichak and Alpert, 2005; Kutiel and Türkeş, 2005; Li *et al.*, 2006; Bueh and Nakamura, 2007).

Teleconnections have been defined as a type of atmospheric circulation that tend to be quasi-stationary to a particular geographic location, generally on the synoptic scale and are usually composed of two or more distant areas of air pressure that have a strong negative correlation to one another (Wallace and Gutzler, 1981; Barnston and Livezey, 1987; Kutiel and Benaroch, 2002; Kutiel and Helfman, 2004). The teleconnections tend to have a strong influence on meteorological parameters in the surrounding regions, and these can have a significant impact on ecology and economy (Hurrell *et al.*, 2003; Trigo *et al.*, 2004). This study focused on the teleconnections located at sea level pressure (SLP) and 500 hPa levels described in Table 1. The teleconnections discussed in this study include the **Mediterranean Oscillation** (**MO**: Conte *et al.*, 1989; Palutikof *et al.*, 1996; Palutikof, 2003; Vicente-Serrano *et al.*, 2009), **North Atlantic Oscillation** (**NAO**: Walker and Bliss, 1934; Wallace and Gutzler, 1981; Barnston and Livezey, 1987; Hurrell, 1995; Davies *et al.*, 1997; Jones *et al.*, 1997; Moulin *et al.*, 1997; Trigo *et al.*, 2002; Hurrell *et al.*, 2003; Vinther *et al.*, 2003; Burroughs, 2007; Vicente-Serrano *et al.*, 2009), **North Sea-Caspian Pattern** (**NCP**: Kutiel and Benaroch, 2002; Kutiel *et al.*, 2002; Kutiel and Türkeş, 2005), **Southern Europe-North Atlantic pattern** (**SENA**: Rogers, 1990; Kutiel and Kay, 1992) and **Western Mediterranean Oscillation** (**WeMO**:

* Correspondence to: J. M. Ciarlo`, Department of Physics, University of Malta, Msida MSD2080, Malta. E-mail: james.ciarlo.06@um.edu.mt

Martin-Vide and Lopez-Bustins, 2006; Vicente-Serrano *et al.*, 2009).

There are several other teleconnections that are likely to have an influence on the Mediterranean Sea, typically the Arctic Oscillation (AO) or Northern Annular Mode (NAM) (Thompson and Wallace, 1998; Ambaum *et al.*, 2001; Tourre *et al.*, 2006), East Atlantic pattern (EA: Wallace and Gutzler, 1981; Esbensen, 1984; Barnston and Livezey, 1987; Kutiel and Kay, 1992), East Atlantic-Western Russia pattern (EAWR: Esbensen, 1984; Barnston and Livezey, 1987; Krichak and Alpert, 2005), Central African-Caspian Oscillation (CACO: Kutiel and Helfman, 2004), and North-Africa/Western Asia pattern (NAWA: Paz *et al.*, 2003; Tourre and Paz, 2004; Tourre *et al.*, 2006) and Scandinavian pattern (SCA: Wallace and Gutzler, 1981; Barnston and Livezey, 1987; Bueh and Nakamura, 2007), however, these patterns were not included due to data storage limitations associated with a significantly larger domain.

All of these teleconnections are located relatively close with respect to each other and some studies (Franzke and Feldstein, 2005; Moore *et al.*, 2013) show that they can have some level of influence on each other. Franzke and Feldstein (2005) discuss the combined effect of the NAO and EA with other teleconnections in the northern Pacific Ocean, and Moore *et al.* (2013) revealed a combined influence of the NAO with the EA as well as with the SCA on the SLP. Other studies have focussed on such behaviour, however, many of these had a low statistical significance, if any, due to the limited number of data points used. Kutiel and Benaroch (2002) had suggested that the NCP was partly responsible for the oscillatory variation in the Mediterranean region implying a possible effect on the MO. Conte *et al.* (1989) found a weak (but not statistically significant) correlation between the MO and the NAO, however, Palutikof (2003) found a statistically significant positive relationship with the exception of the summer months, implying that the two patterns act independently in summer. The WeMO was found to have no statistically significant relationship with EA, and NAO as revealed in a study by Martin-Vide and Lopez-Bustins (2006), however, they also found no statistical significance with EAWR.

Research has shown that variations on the influence of atmospheric circulation patterns can occur across small distances, such as 100 km (Vicente-Serrano *et al.*, 2009), making spatial resolution an important factor in climate simulations. General Circulation Models (GCMs) have been found useful and effective at the representation of large-scale patterns, however, these models do not produce appreciable results for the identification of variability in smaller regions such as southern Europe and the Mediterranean (Conway and Jones, 1998; Trigo and Palutikof, 2001; Li *et al.*, 2006). Some low-resolution GCMs have been used on various occasions to project future changes in the variation and influence of teleconnections (Palutikof *et al.*, 1996; Goodess and Jones, 2002; Trigo *et al.*, 2002; Hurrell *et al.*, 2003; Palutikof, 2003; Bueh and Nakamura, 2007).

For such complex regions applying downscaling techniques at higher resolutions, for example, using dynamical downscaling through Regional Climate Models (RCMs) or statistical downscaling models (Murphy, 1999; Zorita and vonStorch, 1999; Hertig and Jacobeit, 2013), seem more suitable (Conway and Jones, 1998; Trigo and Palutikof, 2001; Li *et al.*, 2006). The community model, RegCM4 (described by Giorgi *et al.*, 2012), is classified as one of the abovementioned RCMs. This model was found to be able to reproduce precipitation and circulation over the Mediterranean and European region (as well as others: Almazroui, 2012; Diro *et al.*, 2012; Giorgi *et al.*, 2012; Ozturk *et al.*, 2012; Diallo *et al.*, 2014; Llopart *et al.*, 2014; Reboita *et al.*, 2014) with small biases, mostly in winter (Giorgi *et al.*, 2012; Fuentes-Franco *et al.*, 2014). Some of these biases were associated to the higher resolution of the model (Grassi *et al.*, 2013). For these parameters, over the Mediterranean and European region, the RegCM4 was found to provide improved results when compared with its predecessor, RegCM3 (Giorgi *et al.*, 2012; Llopart *et al.*, 2014).

The objective of this article is to assess the use of RegCM4 to adequately calculate teleconnection indices. The influence of the indices on each other and the climate in the Mediterranean and surrounding region was also assessed to evaluate the effects of these teleconnections within the model. The details describing the simulation and the method used to calculate the teleconnection indices are presented in Section 2. The analysis is presented and discussed in Section 3, where the indices obtained from the simulation data were compared to data from the 20th Century Reanalysis (20CRv2: Compo *et al.*, 2009). The analysis was composed of a comparison of the index values, their inter-pattern correlations, as well as the effects of the teleconnections on temperature, precipitation and wind. The conclusions of this article were summarized in Section 4.

2. Data and method of analysis

The analysis was based on ensemble mean data obtained from three 1969–1999 climate simulations performed using RegCM4.4-rc8 (version: sr3846 08/07/2013), developed by National Center for Atmospheric Research (NCAR) and maintained by the Earth System Physics of the Abdus Salam International Centre for Theoretical Physics (hereafter referred to as RegCM4; Giorgi *et al.*, 2012). The domain chosen, set at a resolution of 50 km, covered 54°W to 90°E, and 17° to 75°N, to include teleconnections surrounding the Mediterranean Sea listed in Table 1. This domain is larger than the Mediterranean to include regions necessary to describe the teleconnections affecting the basin (while the 20CRv2 domain is larger to fit the RegCM region in the Mercator projection).

The boundary conditions selected for the simulations were the NCEP/NCAR Reanalysis Product version 1 (Kalnay *et al.*, 1996) at 2.5° grid data for the principal driving data and ECHAM5 data (Roeckner *et al.*, 2003;

Table 1. The teleconnections studied described according to altitude and geographical location of the nodes.

	Positive node		Negative node		Reference
	Lat (°N)	Lon (°E)	Lat (°N)	Lon (°E)	
MO	**Algiers**		**Cairo**		Conte *et al.* (1989)
500 hPa	36.4	3.1	30.1	31.4	
NAO	**Gibraltar**		**Reykjavik**		Jones *et al.* (1997)
SLP	36.2	−5.4	64.1	−21.9	
NCP	**North Sea**		**Caspian Sea**		Kutiel and Benaroch (2002)
500 hPa	55.0	0.0/10.0	45.0	50.0/60.0	
SENA	**Piacenza**		**NW Iceland**		Kutiel and Kay (1992)
SLP	45.0	10.0	65.0	−20.0	
WeMO	**Càdiz**		**Padova**		Martin-Vide and Lopez-Bustins (2006)
SLP	36.3	−6.1	45.4	11.8	

Table 2. The selections chosen for the three RegCM4 simulations.

Simulation #	Advection scheme	Pressure gradient force scheme
1	Enabled	Full fields
2	Disabled	Hydrostatic deductions
3	Disabled	Full fields

Roeckner *et al.*, 2006) for sea surface temperatures. Three simulations were run, varying the settings that primarily affect the pressure and wind fields, namely the Semi-Lagrangian Advection Scheme for tracers and humidity and the pressure gradient force scheme as shown in Table 2. This would result in more complex tracer and humidity advection in simulation 1, thereby influencing cloud liquid water formation, radiative forcing and pressure; more complex pressure gradient force calculations in simulation 2, possibly resulting in more turbulent wind flows; less complex but smoother overall general circulation in simulation 3, giving a more streamlined wind flow and less cloud liquid water formation. An ensemble mean constructed from these simulations would reduce pressure and wind uncertainties resulting from intra-variability due to different model configurations. The ensemble mean obtained from these three simulations was used to evaluate the model-derived teleconnection indices; identify which teleconnections are linked together; and classify how the teleconnections influence climatological parameters in the model region.

The reference data used for comparison with the simulation output was the NOAA-CIRES 20th Century Reanalysis version 2 (20CRv2) Ensemble Mean taken at six-hourly intervals for the time period of 1969–1999. This dataset was selected because it provided a complete four-time daily interval for the 1969–1999 time period at a low observation errors (Whitaker *et al.*, 2004; Compo *et al.*, 2006; Compo *et al.*, 2011), ideal for statistically reliable results. The most notable limitations of the 20CRv2 include inhomogeneous observational density during the first half of the 20th century and unreliable precipitation data in the Tropics (Ferguson and Villarini, 2012; Ferguson and Villarini, 2013; Lee and Biasutti, 2014), both of which do not affect this study. The pressure at mean sea level (in Pa) and geopotential heights (GPH) at 500 hPa (in m) data were used to construct reference teleconnection indices for comparison with the RegCM4 teleconnection indices. These indices were then compared with air temperature (in K), U and V-wind (in $m\,s^{-1}$) at the 1000 hPa level, and precipitation rate at the surface (in $kg\,m^{-2}\,s^{-1}$) using correlation field plots for temperature and precipitation, and similar correlation field plots which included vectors (henceforth referred to as 'correlation vector fields') for the winds to account for the effect on direction.

The state of a particular teleconnection is quantified with the use of an index, which relates the difference between the nodes based on the statistical z-test (Walker and Bliss, 1934; Wallace and Gutzler, 1981; Kutiel and Helfman, 2004). The generalized method described in Equations (1)–(3), was identified and applied to each teleconnection, following techniques used by Conte *et al.* (1989), Kutiel and Benaroch (2002) and Kutiel and Helfman (2004) to provide index values specific for the teleconnections described in these studies. However, as both the RegCM and 20CRv2 datasets were gridded, the data for each node was taken as a single grid point for every representative set of the coordinates shown in Table 1. Such station-based indices were found to be better at representing atmospheric forcing when using data with a greater atmospheric variability (Criado-Aldeanueva and Soto-Navarro, 2013). Thus, the station-based method was chosen in preference to principal component based techniques as the high atmospheric variability resulting from the four-time daily RegCM4 data would provide a better representation of the teleconnection effects.

The data for the period 1969–1999 was used to calculate the index value, z of time step i and month j, as represented in Equation (1). Diff_{ij} describes the difference between the positive (largest pressure anomalies) and negative (the smallest pressure anomalies) nodes of the same time step and month, as shown in Equation (2). The quantity, $\overline{\mathrm{Diff}_j}$ represents the average of all Diff_{ij} values associated with a month j, irrespective of years, thereby resulting in 12 climate averages in the entire time period. Lastly,

$\sigma_j(\mathrm{Diff}_{ij})$, given in Equation (3), is the standard deviation for the month j, where N is the number of time steps considered in the expression.

$$z_{ij} = \left(\mathrm{Diff}_{ij} - \overline{\mathrm{Diff}_j}\right) / \sigma_j\left(\mathrm{Diff}_{ij}\right) \quad (1)$$

$$\mathrm{Diff}_{ij} = (\text{Positive node})_{ij} - (\text{Negative node})_{ij} \quad (2)$$

$$\sigma_j\left(\mathrm{Diff}_{ij}\right) = \sqrt{(1/N)\sum_{i=0}^{i=N}\left(\mathrm{Diff}_{ij} - \overline{\mathrm{Diff}_j}\right)^2} \quad (3)$$

3. Analysis and results

3.1. Teleconnection indices

The first objective of the analysis was to compare the teleconnection indices obtained from the ensemble RegCM4 simulation output with those obtained from the 20CRv2 data. The SLP and 500 hPa GPH data were extracted from the grid points representing the nodes described in Table 1, and the method described in Section 2 was used to calculate the teleconnection indices from both the RegCM4 and 20CRv2 data. A simple comparison of the time series for the monthly moving average of the teleconnection indices (Figures S1–S3, Supporting Information) between 1969 and 1999 reveals a great similarity between both the RegCM4 and 20CRv2-derived indices. However, this is not enough to compare the relative differences between each pair of time series and evaluate whether the simulation results deviate significantly from the reanalysis data.

The teleconnection indices constructed from the RegCM4 data were thus compared with those constructed from the 20CRv2 data using Pearson correlation across the 1969–1999 time period. The resulting correlation coefficients are presented in Table 3; these were all found to be positive and statistically significant to the 0.001 level, with the NAO and SENA having coefficients closest to 1. The time series shown in Figures S1–S3 visualize the different values obtained by the Pearson correlation. PDFs shown in Figures 1–3, were constructed to compare the distributions of the teleconnection indices. These plots were mostly identical with very similar means and standard deviations, showing that the results for the indices were reliable. Therefore, despite the fact that the coefficients for MO, NCP and WeMO deviated further from a value of 1, these results were deemed acceptable as the objective of a climate simulation is to obtain long-term projections of the climatology rather than short-term day-to-day forecasts.

3.2. Inter-pattern analysis

As the influence of teleconnection patterns extends over large distances, and these teleconnections are relatively close to each other, it is likely that they would interact as suggested by Franzke and Feldstein (2005) and Moore *et al.* (2013). Such interactions may cause interference or strengthen the effect of other teleconnections. The nature of inter-pattern correlation was quantified using a Pearson correlation analysis on the 20CRv2-derived indices and the RegCM4-derived indices as shown in Tables 4 and 5, respectively; the latter also shows the absolute error of these values when compared with the values of Table 4, as described by Abramowitz and Stegun (1972).

Table 3. Pearson correlation coefficients for RegCM4-derived indices compared with 20CRv2-derived indices. All coefficients were statistically significant to the 0.001 level.

	MO	NAO	NCP	SENA	WeMO
R	0.632	0.840	0.657	0.797	0.610

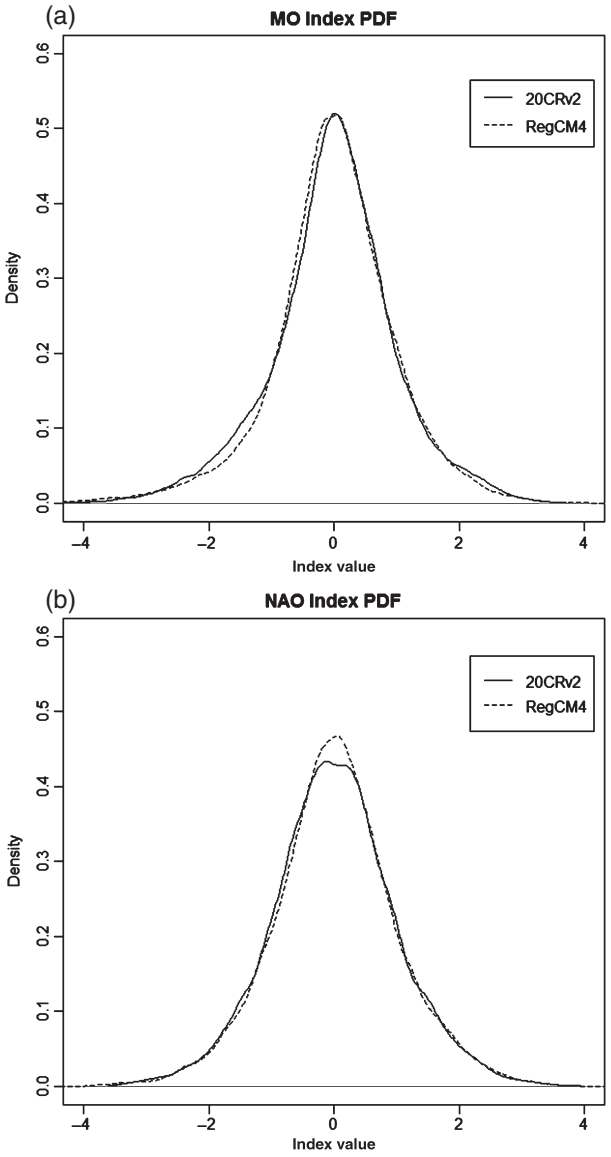

Figure 1. MO (a) and NAO (b) teleconnection index PDFs for 20CRv2 and RegCM4-derived indices for the period of 1969–1999.

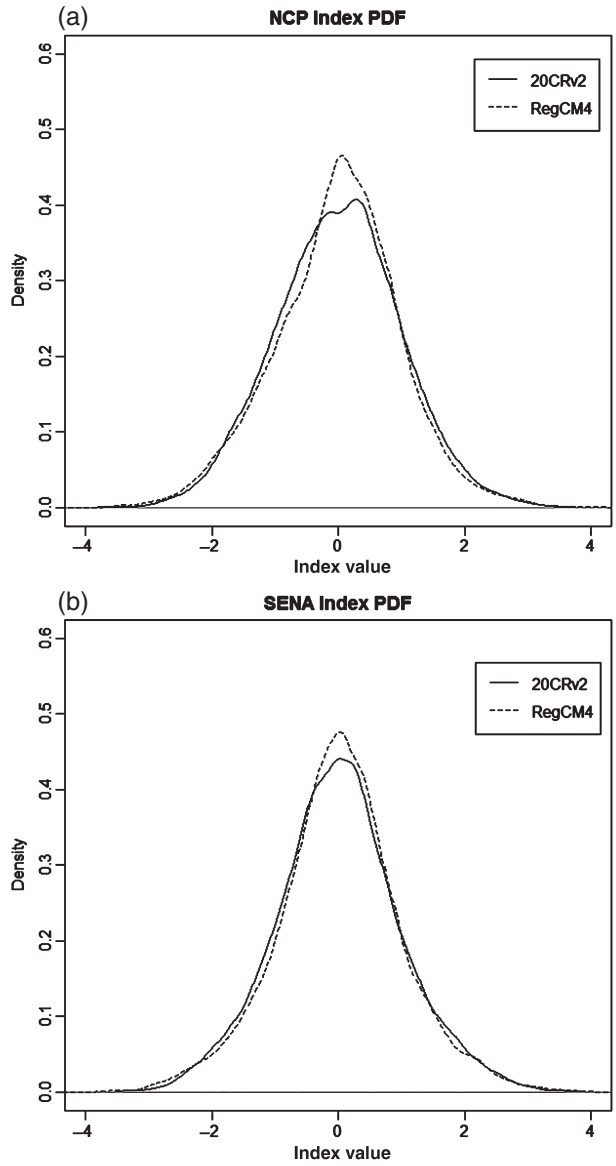

Figure 2. NCP (a) and SENA (b) teleconnection index PDFs for 20CRv2 and RegCM4-derived indices for the period of 1969–1999.

It is important to note that despite the similarities, there were a few minor differences between the data presented in Tables 4 and 5. Rogers (1990) had described a similarity between the NAO and SENA teleconnections, which in this analysis was quantified at a value of 0.859. This is similar to the concept described by Kutiel and Benaroch (2002) where the NCP and EAWR may be representations of the same teleconnection, even though Barnston and Livezey (1987) describe the EAWR with a third weaker pole which is disregarded by Krichak and Alpert (2005) for the NCP. However, the remaining inter-pattern correlations of NAO and SENA were very different; therefore one cannot describe them as different indices of the same teleconnection.

The NCP and MO were found to have a low correlation of 0.041/0.161 (20CRv2/RegCM4, respectively), which could contradict the link suggested by Kutiel and Benaroch (2002). A weak correlation of 0.206/0.306 between the

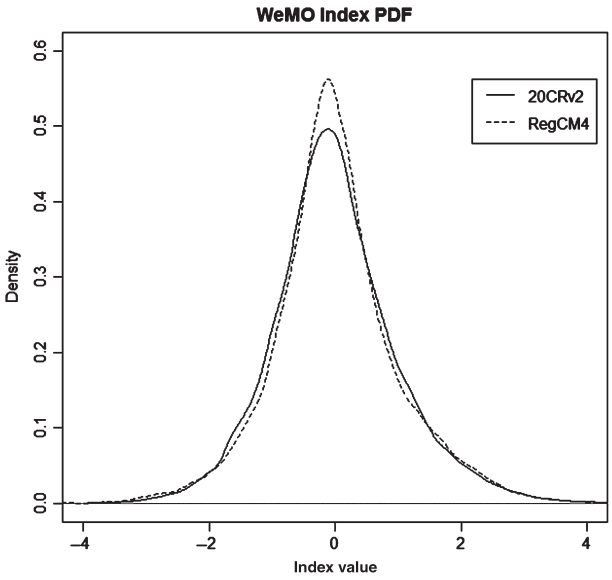

Figure 3. WeMO teleconnection index PDFs for 20CRv2 and RegCM4-derived indices for the period of 1969–1999.

MO and NAO agrees with the results of Conte *et al.* (1989) and Palutikof (2003). The relationship between the WeMO and NAO was found to be very low at 0.094/0.097, which explains why Martin-Vide and Lopez-Bustins (2006) observed no interaction between these patterns. The NCP and WeMO had the highest negative correlation, with a value of −0.553, and together with the MO to WeMO and the SENA to WeMO relationship, describe a degree of interference in the effects of each of these patterns with the WeMO, possibly as a result of the proximity of one pattern's positive node with the other's negative node.

Comparing Tables 4 and 5, one can note that out of 10 inter-pattern correlations, the RegCM4 reproduces 5 interactions with absolute errors smaller than 0.05, 2 interactions with errors smaller than 0.07 and 3 with errors smaller than 0.15. One should also note that all the correlation values obtained by the RegCM4-derived indices are larger in magnitude that those from the 20CRv2-derived indices. As the process of downscaling data to a higher resolution, which occurs within a RCM, increases the detail of the parameter dynamics, it is possible that the more highly resolved points used to calculate the teleconnection indices reveal a more pronounced interaction (as suggested by Grassi *et al.*, 2013), thereby resulting in the observed differences in Tables 4 and 5.

3.3. Significance of correlation field plots

The most sought after effect of a teleconnection is how the state of that teleconnection can affect the climate of adjacent regions. In order to better understand their nature and the reliability of the model to reproduce the expected teleconnection indices, the influence on air temperature, precipitation and wind was investigated with the use of correlation field plots. For these plots, the correlation

Table 4. The Pearson correlation coefficients between the 20CRv2-derived indices. All coefficients were statistically significant to the 0.001 level.

NCEP	MO	NAO	NCP	SENA	WeMO
MO	1	0.206	0.041	0.230	−0.100
NAO		1	0.067	0.859	0.094
NCP			1	0.342	−0.553
SENA				1	−0.388
WeMO					1

Table 5. The Pearson correlation coefficients between the RegCM4-derived indices and absolute error (in italics) of these values compared with the 20CRv2 correlations. All coefficients were statistically significant to the 0.001 level.

RegCM4	MO	NAO	NCP	SENA	WeMO
MO	1	0.306	0.161	0.353	−0.122
NAO	*0.100*	1	0.104	0.845	0.097
NCP	*0.120*	*0.037*	1	0.406	−0.596
SENA	*0.123*	*0.014*	*0.064*	1	−0.439
WeMO	*0.022*	*0.003*	*0.043*	*0.051*	1

coefficient, R is regarded as significant to the 0.05 level if the magnitude of R corresponds to the value obtained from the expression described by Burroughs (2007), shown in Equation (4).

$$|R| \geq 1.96/\sqrt{N} \tag{4}$$

The quantity, N represents the number of samples (44 921), thereby making the threshold, $|R| = 0.009$. Therefore, correlation coefficients, with magnitudes smaller than 0.009, would be regarded as non-significant. However, when considering the problem of multiplicity (Katz and Brown, 1991) a confidence level of 0.05 for the number of hypothesis assumed in the correlation field (108×170) requires a p-value of 2.723×10^{-6} using the Bonferroni adjustment. As a result of this, using t-statistics (Cohen *et al.*, 2003), the constant of 1.96, presented in Equation (4), is replaced with 4.83, as shown in Equation (5), resulting in a correlation threshold, $|R|$ of 0.023, with a p-value of 1.087×10^{-6}.

$$|R| \geq 4.83/\sqrt{N} \tag{5}$$

However, Katz and Brown (1991) also explained the need to account for autocorrelation of the parameters, by dividing the degrees of freedom with a 'variance inflation factor', in order to obtain the correct p-value. This is dependent on the autocorrelation coefficient of every individual time series, therefore after accounting for the maximum and minimum possible autocorrelations, a number of factors were considered for the p-value. In these cases, when considering Equation (5), the threshold value, $|R|$ varied between 0.023 and 0.028. However, the smallest value for the contours presented in Sections 3.4 to 3.6 is 0.1, therefore, any correlation coefficient of magnitude higher than 0.1, in Figures 4–6, were considered to be statistically significant to the 0.05 level.

3.4. Influence on temperature

The NAO depends on the Icelandic Low and Azores High (Davies *et al.*, 1997; Moulin *et al.*, 1997; Hurrell *et al.*, 2003), as a result, the strongest influence of the teleconnection is around these two locations (Figure 4). Similarly, all teleconnections displayed the strongest influence around the areas of their respective nodes. The influence of the remaining teleconnections on temperature is shown in the Supporting Information. The MO (Figure S4) and NCP (Figure S5) displayed a positive correlation with the temperature surrounding the geographical location in relative proximity to the positive poles and negative correlations with the areas surrounding the negative poles; the NAO, SENA and WeMO (Figures 4, S6 and S7, respectively) however, displayed the opposite of this. This is probably caused by the influence of the teleconnection on circulation (described in Section 3.6), as warmer air from the South is carried North during the positive index phase, on the East side of the negative pole. One can also note that both the NCP and MO affect temperature in a similar way inside the Mediterranean basin, which would explain the possible link between the two patterns described by Kutiel and Benaroch (2002). However, the low influence of the NCP on the East and West side of the basin, and the lack of influence by the MO near the North and Caspian Seas, explains why this interaction was so low in Section 3.2.

3.5. Influence on precipitation

Despite the different influence on temperature, all teleconnections revealed a positive correlation with precipitation in the areas close to the negative nodes, and vice versa for the positive nodes. For example, the MO, with the positive node in the West of the Mediterranean and the negative node in the East, shows a negative correlation with the precipitation in the West and positive in the East. Both the MO and NCP displayed similar 'seesaw' behaviour over the Mediterranean as described by Conte *et al.* (1989); this, together with the correlation revealed in Section 3.2, shows a significant but low correlation between the MO and NCP (Figures 5 and S9), previously suggested by Kutiel and Benaroch (2002).

The NAO (Figure S8) and SENA (Figure S10) displayed a positive correlation on precipitation surrounding the area of the Icelandic low and the northernmost parts of Europe while displaying a negative relationship over the Azores, Spain and part of the western Mediterranean, similar to the description provided by Hurrell (1995). The remaining teleconnections appeared to have a greater influence over precipitation in the Mediterranean and Europe than the NAO and SENA. The NCP (Figure S9) had a negative correlation that dominated over northern Europe which extended further, however weakly, towards the Mediterranean according to the RegCM data. While the influence of the MO was focused over the Mediterranean, the influence of the WeMO (Figure S11) extended over most of Europe and the Mediterranean with a positive correlation and a negative correlation over Spain and the Azores.

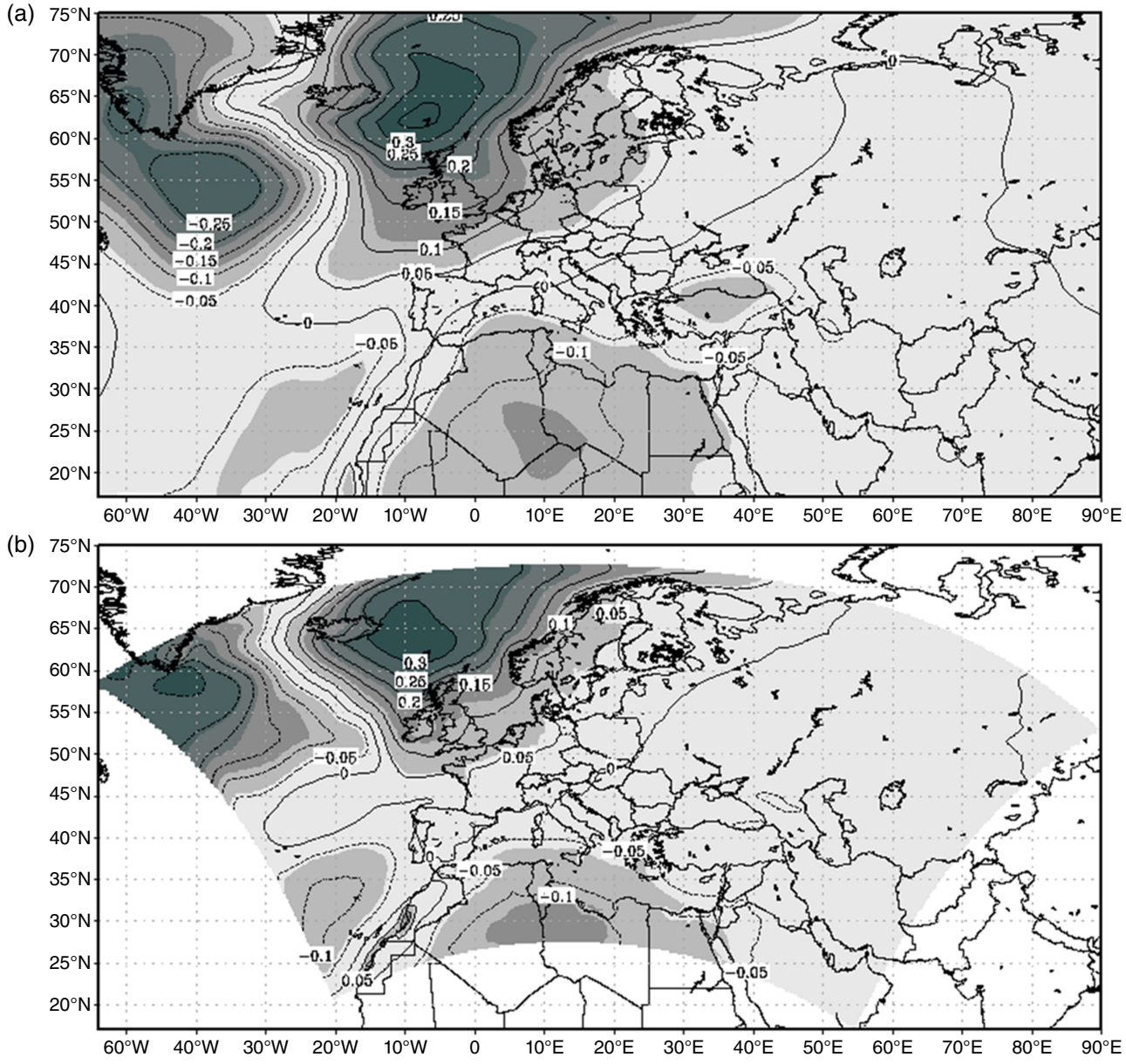

Figure 4. Correlation field map for the period of 1969–1999 between the NAO index and air temperature (K) at 1000 hPa for 20CRv2 (a) and RegCM4 (b). Correlations of magnitudes higher than 0.1 are statistically significant to the 0.05 level.

3.6. Influence on winds

Also, as expected, at the positive nodes of all teleconnections during the positive index phase, winds (at 1000 hPa) are influenced towards a clockwise motion around the nodes, and conversely, anti-clockwise around the negative nodes, further strengthening the flow between the two nodes, for example for the NCP (Figure 6) as described by Kutiel and Benaroch (2002). Understandably, the behaviour revealed in these 'correlation vector fields', is inverted during the negative index phases of the teleconnections. The teleconnection influence on winds for the MO, NAO, SENA and WeMO (Figures S12–S15) are shown in the Supporting Information, all of which have shown a strong influence on winds over the Mediterranean.

Each Figure shows the correlation fields obtained from 20CRv2 data and the RegCM4 simulation; these have revealed very similar results that support the use of the RegCM4 model for such studies. It is important to stress the issue that the plots are not and cannot be identical as the resolution of the 20CRv2 and RegCM4 data are very different, however, the more highly resolved results from the RegCM4 data further justifies the use of the model for the projection of teleconnection indices and their effects. With these correlation fields, one can provide an understanding of the extent and nature of influence of each teleconnection in relation to temperature, precipitation and wind.

4. Summary and conclusions

This article has utilized the index calculation techniques presented in a number of studies to obtain a generalized

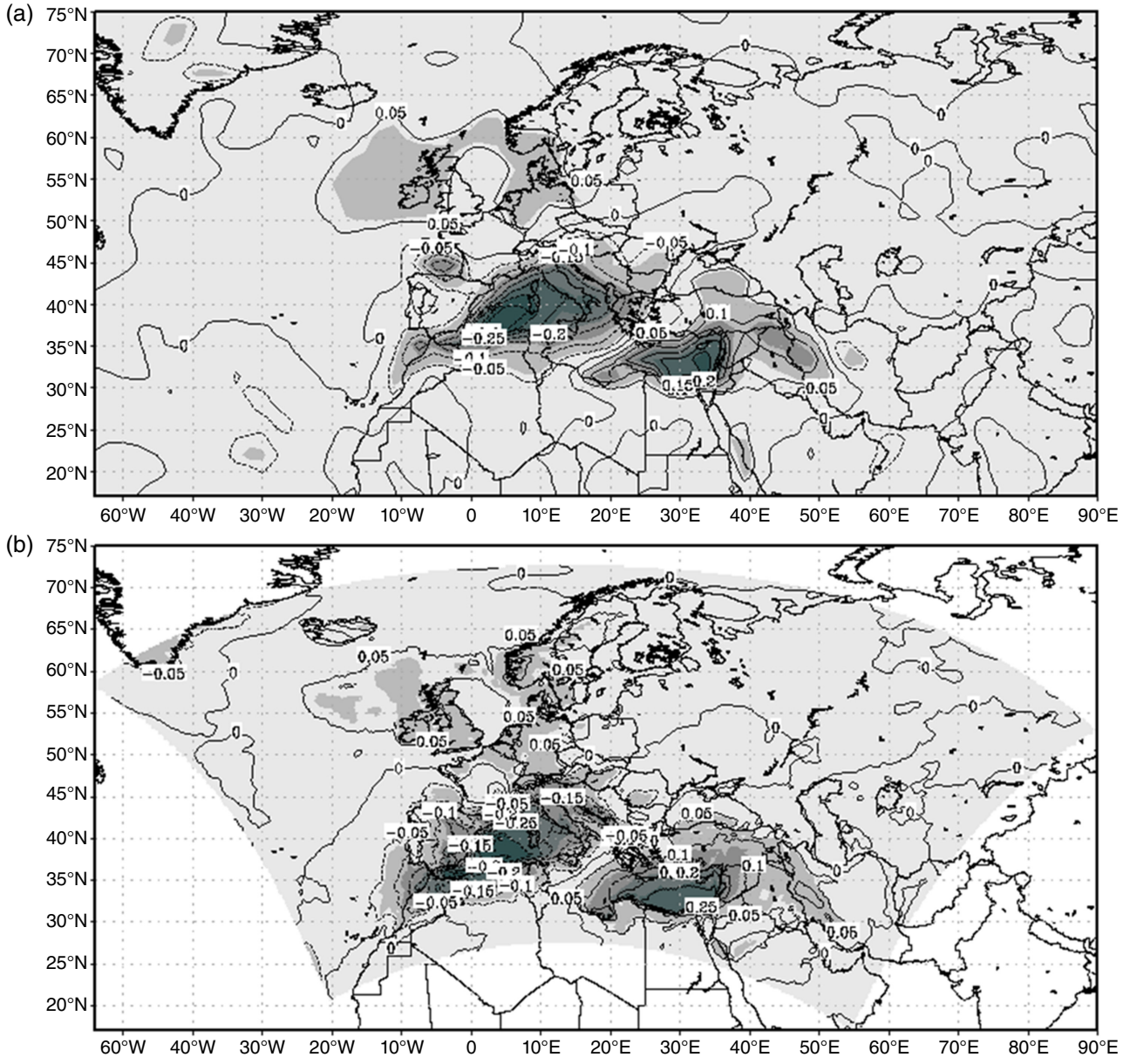

Figure 5. Correlation field map for the period of 1969–1999 between the MO index and precipitation rate ($kg\,m^{-2}\,s^{-1}$) for 20CRv2 (a) and RegCM4 (b). Correlations of magnitudes higher than 0.1 are statistically significant to the 0.05 level.

index for five teleconnections in and around the Mediterranean. When compared with previous studies, this study uses a very large data set (with over 44 000 time steps) to explore the interaction between five teleconnections by comparing the indices of these teleconnections as well as mapping their effects on temperature, precipitation and wind.

This study has revealed that the teleconnection index PDFs calculated from the RegCM4 data were almost identical to those obtained from the 20CRv2. The correlation coefficients also show that the temporal variation of the modelled indices are reliable and the analysis revealed a statistically significant correlation for all teleconnections, with the highest coefficients observed for the NAO and SENA. Therefore, one can state that the RegCM4 can reproduce reliable teleconnections.

Most of the inter-pattern correlations were found to have small errors, however, the error in the interaction of MO with NCP and SENA was greater than 0.1, although one should also note that the nodes of these patterns are found in complex orographic regions resulting in a larger difference as a result of downscaling. The MO to NCP interaction was suggested by Kutiel and Benaroch (2002) due to the 'seesaw' behaviour displayed by the MO and NCP over the Mediterranean, which was also observed in this study and hence suggests a relationship between the two patterns. It is possible that the difference observed was a result of the higher resolution of the RegCM4 data as suggested by Grassi *et al.* (2013). The model mechanism was an unlikely cause of these differences, as the ensemble mean, which included combinations for advection and pressure gradient force, would have diminished such errors. In such

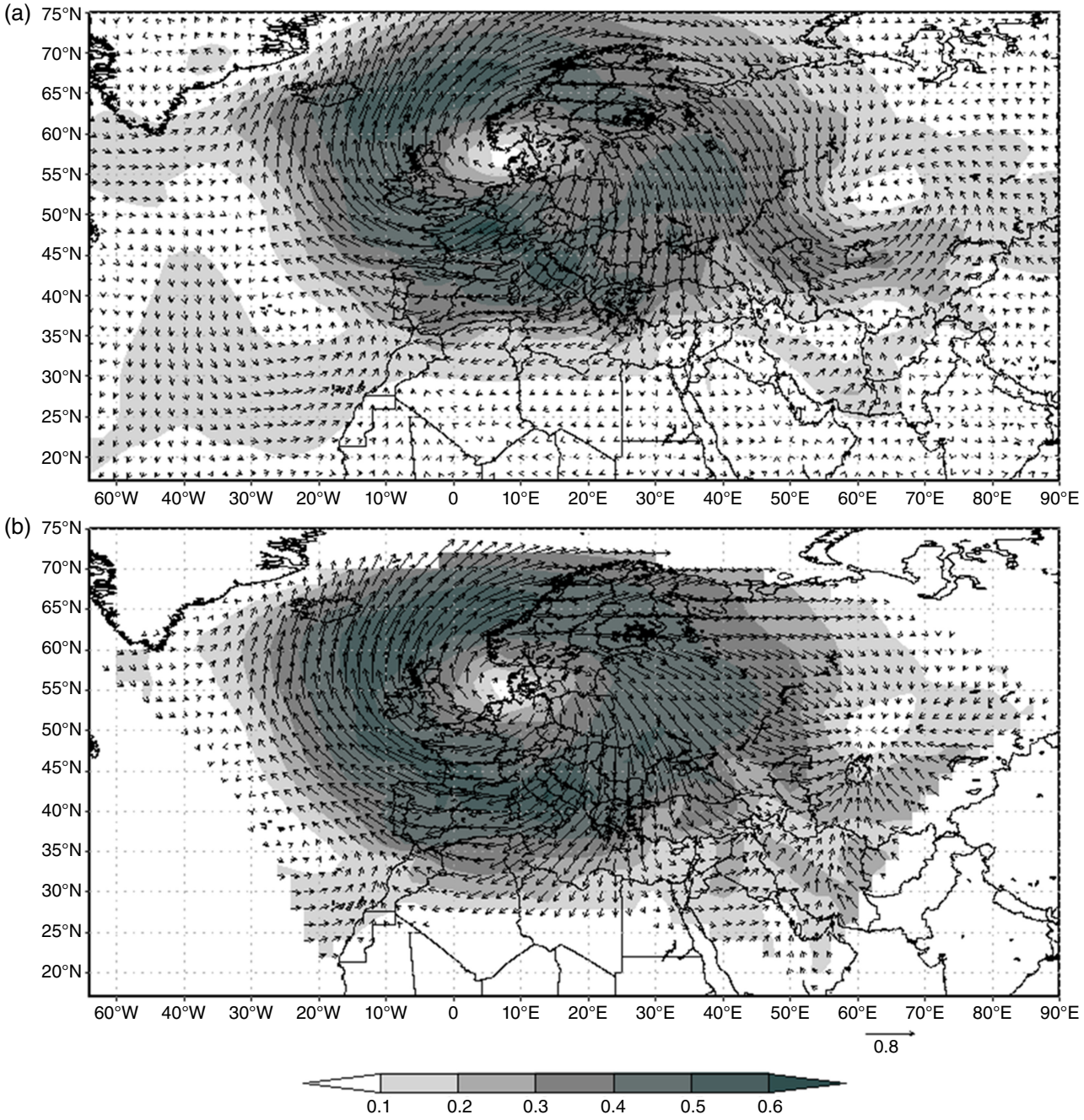

Figure 6. Correlation field map for the period of 1969–1999 between the NCP index and wind speed ($m\,s^{-1}$) for 20CRv2 (a) and RegCM4 (b). The arrows describes the vector component, and the shading describes the magnitude of the correlation coefficient, representing the change in wind effected by the teleconnection. Correlations of magnitudes higher than 0.1 are statistically significant to the 0.05 level.

a case, the higher correlation observed between the MO and NCP in the RegCM4 data corroborates with the studies of Kutiel and Benaroch (2002).

Rogers (1990) suggested a strong relationship between the NAO and SENA, and that the latter is a part of the NAO teleconnection. Despite the high correlation observed between these patterns which reinforces the strong relationship between the phenomena, the difference in their influence on the surrounding region and patterns shows that they are not the same pattern. The high correlation coefficient observed was probably a result of the proximity between the nodes of the patterns, most notably because of the Icelandic node. The inter-pattern correlations corroborate the positive correlation coefficient between MO and NAO observed by Conte *et al.* (1989) and Palutikof (2003). Although a statistically significant correlation between WeMO and NAO was found, this value is very low and explains the lack of significance observed by Martin-Vide and Lopez-Bustins (2006).

The 20CRv2 and RegCM4 correlation fields were comparable, revealing small deviations from the driving data and thereby increasing the confidence of possible long-term projections. These results contrast with those from GCMs and other low-resolution models used in

the past and therefore, it can be stated with reasonable confidence that RegCM4 simulation data could be applied for future climatological projections of these five teleconnections and their regional atmospheric effects, with the highest confidence associated with the NAO and SENA. It is possible that the technique presented in this article could be applied to different teleconnections and RCMs, however, an extensive evaluation would be required.

Acknowledgements

This research has been carried out using computational facilities procured through the European Regional Development Fund, Project ERDF-080 'A supercomputing laboratory for the University of Malta' (http://www.um.edu.mt/research/scienceeng/erdf_080). Support for the Twentieth Century Reanalysis Project dataset was provided by the U.S. Department of Energy, Office of Science Innovative and Novel Computational Impact on Theory and Experiment (DOE INCITE) program, and Office of Biological and Environmental Research (BER), and by the National Oceanic and Atmospheric Administration Climate Program Office.

The authors would like to thank the Department of Physics at the University of Malta for providing funding for this research, together with Alessio Magro for the support provided with the supercomputing facility, Jackson Said for his valuable suggestions and constructive discussions, as well as Lino Sant from the Department of Statistics and Operations Research at the University of Malta for his assistance in the use of statistical analysis techniques. They would also like to thank Xunqiang Bi, Stefano Cozzini, and Graziano Giuliani from the Abdus Salam International Centre for Theoretical Physics for the technical support provided with the use of the RegCM4.

Supporting Information

The following supporting information is available as part of the online article:

Appendix S1. Teleconnection timeseries and additional correlation field maps.

Figure S1. MO index monthly moving average time series from 1969 to 1999.

Figure S2. NAO (a) and NCP (b) index monthly moving average time series from 1969 to 1999.

Figure S3. SENA (a) and WeMO (b) index monthly moving average time series from 1969 to 1999.

Figure S4. Correlation field map for the period of 1969–1999 between the MO index and air temperature (K) at 1000 hPa for 20CRv2 (a) and RegCM4 (b). Correlations of magnitudes higher than 0.1 are statistically significant to the 0.05 level.

Figure S5. Correlation field map for the period of 1969–1999 between the NCP index and air temperature (K) at 1000 hPa for 20CRv2 (a) and RegCM4 (b). Correlations of magnitudes higher than 0.1 are statistically significant to the 0.05 level.

Figure S6. Correlation field map for the period of 1969–1999 between the SENA index and air temperature (K) at 1000 hPa for 20CRv2 (a) and RegCM4 (b). Correlations of magnitudes higher than 0.1 are statistically significant to the 0.05 level.

Figure S7. Correlation field map for the period of 1969–1999 between the WeMO index and air temperature (K) at 1000 hPa for 20CRv2 (a) and RegCM4 (b). Correlations of magnitudes higher than 0.1 are statistically significant to the 0.05 level.

Figure S8. Correlation field map for the period of 1969–1999 between the NAO index and precipitation rate ($kg\,m^{-2}\,s^{-1}$) for 20CRv2 (a) and RegCM4 (b). Correlations of magnitudes higher than 0.1 are statistically significant to the 0.05 level.

Figure S9. Correlation field map for the period of 1969–1999 between the NCP index and precipitation rate ($kg\,m^{-2}\,s^{-1}$) for 20CRv2 (a) and RegCM4 (b). Correlations of magnitudes higher than 0.1 are statistically significant to the 0.05 level.

Figure S10. Correlation field map for the period of 1969–1999 between the SENA index and precipitation rate ($kg\,m^{-2}\,s^{-1}$) for 20CRv2 (a) and RegCM4 (b). Correlations of magnitudes higher than 0.1 are statistically significant to the 0.05 level.

Figure S11. Correlation field map for the period of 1969–1999 between the WeMO index and precipitation rate ($kg\,m^{-2}\,s^{-1}$) for 20CRv2 (a) and RegCM4 (b). Correlations of magnitudes higher than 0.1 are statistically significant to the 0.05 level.

Figure S12. Correlation field map for the period of 1969–1999 between the MO index and wind speed ($m\,s^{-1}$) for 20CRv2 (a) and RegCM4 (b). The arrows describes the vector component, and the shading describes the magnitude of the correlation coefficient, representing the change in wind affected by the teleconnection. Correlations of magnitudes higher than 0.1 are statistically significant to the 0.05 level.

Figure S13. Correlation field map for the period of 1969–1999 between the NAO index and wind speed ($m\,s^{-1}$) for 20CRv2 (a) and RegCM4 (b). The arrows describes the vector component, and the shading describes the magnitude of the correlation coefficient, representing the change in wind affected by the teleconnection. Correlations of magnitudes higher than 0.1 are statistically significant to the 0.05 level.

Figure S14. Correlation field map for the period of 1969–1999 between the SENA index and wind speed ($m\,s^{-1}$) for 20CRv2 (a) and RegCM4 (b). The arrows describes the vector component, and the shading describes the magnitude of the correlation coefficient, representing the change in wind affected by the teleconnection. Correlations of magnitudes higher than 0.1 are statistically significant to the 0.05 level.

Figure S15. Correlation field map for the period of 1969–1999 between the WeMO index and wind speed ($m\,s^{-1}$) for 20CRv2 (a) and RegCM4 (b). The arrows describes the vector component, and the shading describes the magnitude of the correlation coefficient, representing

the change in wind affected by the teleconnection. Correlations of magnitudes higher than 0.1 are statistically significant to the 0.05 level.

References

Abramowitz M, Stegun IA. 1972. *Handbook of Mathematical Functions: with Formulas, Graphs, and Mathematical Tables*. Dover Publications, Inc.: New York, NY.

Ackerman SA, Knox JA. 2011. *Meteorology: Understanding the Atmosphere*, 3rd edn. Jones & Bartlett Learning: Sudbury, Canada.

Almazroui M. 2012. Dynamical downscaling of rainfall and temperature over the Arabian Peninsula using RegCM4. *Clim. Res.* **52**: 49–62, doi: 10.3354/cr01073.

Ambaum MHP, Hoskins BJ, Stephenson DB. 2001. Arctic Oscillation or North Atlantic Oscillation? *J. Clim.* **14**: 3495–3507, doi: 10.1175/1520-0442(2001)014<3495:AOONAO>2.0.CO;2.

Barnston AG, Livezey RE. 1987. Classification, seasonality and persistence of low-frequency atmospheric circulation patterns. *Mon. Weather Rev.* **115**: 1083–1126, doi: 10.1175/1520-0493(1987)115<1083:CSAPOL>2.0.CO;2.

Bauer L, Morikawa GK. 1976. Stability of rectilinear geostrophic vortices in stationary equilibrium. *Phys. Fluids* **19**: 929–942.

Bueh C, Nakamura H. 2007. Scandinavian pattern and its climatic impact. *Q. J. R. Meteorol. Soc.* **133**: 2117–2131, doi: 10.1002/qj.173.

Burroughs WJ. 2007. *Climate Change: A Multidisciplinary Approach*, 2nd edn. Cambridge University Press: New York, NY.

Christoforou P, Hameed S. 1997. Solar cycle and the Pacific 'centers of action'. *Geophys. Res. Lett.* **24**: 293–296.

Cohen J, Cohen P, West SG, Aiken LS. 2003. *Applied Multiple Regression/Correlation Analysis for the Behavioral Sciences*, 3rd edn. Lawrence Earlbaum Associates: Mahwah, NJ.

Compo GP, Whitaker JS, Sardeshmukh PD. 2006. Feasibility of a 100 year reanalysis using only surface pressure data. *Bull. Am. Meteorol. Soc.* **87**: 175–190.

Compo GP, Whitaker JS, Sardeshmukh PD, Matsui N, Allan RJ, Yin X, Gleason BE, Vose RS, Rutledge G, Bessemoulin P, Bronnimann S, Brunet M, Crouthamel RI, Grant AN, Groisman PY, Jones PD, Kruk MC, Kruger AC, Marshall GJ, Maugeri M, Mok HY, Nordli O, Ross TF, Trigo RM, Wang XL, Woodruff SD, Worley SJ. 2009. *NOAA CIRES Twentieth Century Global Reanalysis Version 2*. Research Data Archive at the National Center for Atmospheric Research, Computational and Information Systems Laboratory. 10.5065/D6QR4V37.

Compo GP, Whitaker JS, Sardeshmukh PD, Matsui N, Allan RJ, Yin X, Gleason BE, Vose RS, Rutledge G, Bessemoulin P, Brönnimann S, Brunet M, Crouthamel RI, Grant AN, Groisman PY, Jones PD, Kruk MC, Kruger AC, Marshall GJ, Maugeri M, Mok HY, Nordli Ø, Ross TF, Trigo RM, Wang XL, Woodruff SD, Worley SJ. 2011. The twentieth century reanalysis project. *Q. J. R. Meteorol. Soc.* **137**: 1–28, doi: 10.1002/qj.776.

Conte M, Giuffrida A, Tedesco S. 1989. The Mediterranean oscillation: impact on precipitation and hydrology in Italy. In *Conference on Climate and Water*. Helsinki, Finland, 11–15 September 1989. The Publications of the Academy of Finland: Helsinki.

Conway D, Jones PD. 1998. The use of weather types and air flow indices for GCM downscaling. *J. Hydrol.* **212–213**: 348–361.

Criado-Aldeanueva F, Soto-Navarro FJ. 2013. The Mediterranean Oscillation teleconnection index: station-based versus principal component paradigms. *Adv. Meteorol.* **2013**: 1–10.

Davies T, Kelly PM, Osborn T. 1997. Chapter 2: Explaining the climate of the British Isles. In *Climates of the British Isles: Present, Past and Future*, Hulme M, Barrow E (eds). Routledge: London.

Diallo I, Giorgi F, Sukumaran S, Stordal F, Giuliani G. 2014. Evaluation of RegCM4 driven by CAM4 over Southern Africa: mean climatology, interannual variability and daily extremes of wet season temperature and precipitation. *Theor. Appl. Climatol.,* doi: 10.1007/s00704-014-1260-6.

Diro GT, Rauscher SA, Giorgi F, Tompkins AM. 2012. Sensitivity of seasonal climate and diurnal precipitation over Central America to land and sea surface schemes in RegCM4. *Clim. Res.* **52**: 31–48, doi: 10.3354/cr01049.

Esbensen SK. 1984. A comparison of intermonthly and interannual teleconnections in the 700 mb geopotential height field during the Northern Hemisphere winter. *Mon. Weather Rev.* **112**: 2016–2032, doi: 10.1175/1520-0493(1984)112<2016:ACOIAI>2.0.CO;2.

Ferguson CR, Villarini G. 2012. Detecting inhomogeneities in the Twentieth Century Reanalysis over the central United States. *J. Geophys. Res.* **117**: D05123, doi: 10.1029/2011JD016988.

Ferguson CR, Villarini G. 2013. An evaluation of the statistical homogeneity of the Twentieth Century Reanalysis. *Clim. Dyn.* **42**: 2841–2866, doi: 10.1007/s00382-013-1996-1.

Franzke C, Feldstein SB. 2005. The continuum and dynamics of Northern Hemisphere teleconnection patterns. *J. Atmos. Sci.* **62**: 3250–3267.

Fuentes-Franco R, Coppola E, Giorgi F, Pavia EG, Diro GT, Graef F. 2014. Inter-annual variability of precipitation over Southern Mexico and Central America and its relationship to sea surface temperature from a set of future projections from CMIP5 GCMs and RegCM4 CORDEX simulations. *Clim. Dyn.,* doi: 10.1007/s00382-014-2258-6.

Giorgi F, Coppola E, Solmon F, Mariotti L, Sylla MB, Bi X, Elguindi N, Diro GT, Nair V, Giuliani G, Turuncoglu UU, Cozzini S, Güttler I, O'Brien TA, Tawfik AB, Shalaby A, Zakey AS, Steiner AL, Stordal F, Sloan LC, Brankovic C. 2012. RegCM4: model description and preliminary tests over multiple CORDEX domains. *Clim. Res.* **52**: 7–29, doi: 10.3354/cr01018.

Goodess CM, Jones PD. 2002. Links between circulation and changes in the characteristics of Iberian rainfall. *Int. J. Climatol.* **22**: 1593–1615.

Grassi B, Redaelli G, Visconti G. 2013. Arctic Sea ice reduction and extreme climate events over the Mediterranean region. *J. Clim.* **26**: 10101, doi: 10.1175/JCLI-D-12-00697.1.

Hertig E, Jacobeit J. 2013. A novel approach to statistical downscaling considering nonstationarities: application to daily precipitation in the Mediterranean area. *J. Geophys. Res.-Atmos.* **118**: 520–533.

Hurrell JW. 1995. Decadal trends in the North Atlantic Oscillation: regional temperatures and precipitation. *Science* **269**: 676–679.

Hurrell JW, Kushnir Y, Ottersen G, Visbeck M. 2003. An overview of the North Atlantic Oscillation. In *The North Atlantic Oscillation: Climatic Significance and Environmental Impact*, Hurrell JW, Kushnir Y, Ottersen G, Visbeck M (eds). American Geophysical Union: Washington, DC.

Jones PD, Jonsson T, Wheeler D. 1997. Extension to the North Atlantic oscillation using early instrumental pressure observations from Gibraltar and south-west Iceland. *Int. J. Climatol.* **17**: 1433–1450, doi: 10.1002/(sici)1097-0088(19971115)17:13<1433::aid-joc203>3.0.co;2-p.

Kalnay E, Kanamitsu M, Kistler R, Collins W, Deaven D, Gandin L, Iredell M, Saha S, White G, Woollen J, Zhu Y, Leetmaa A, Reynolds R, Chelliah M, Ebisuzaki W, Higgins W, Janowiak J, Mo KC, Ropelewski C, Wang J, Jenne R, Joseph D. 1996. The NCEP/NCAR 40-year reanalysis project. *Bull. Am. Meteorol. Soc.* **77**: 437–471, doi: 10.1175/1520-0477(1996)077<0437:TNYRP>2.0.CO;2.

Katz RW, Brown BG. 1991. The problem of multiplicity in research on teleconnections. *Int. J. Climatol.* **11**: 505–513.

Krichak SO, Alpert P. 2005. Decadal trends in the East Atlantic-West Russia pattern and Mediterranean precipitation. *Int. J. Climatol.* **25**: 183–192.

Kutiel H, Benaroch Y. 2002. North Sea-Caspian Pattern (*NCP*) – an upper level atmospheric teleconnection affecting the Eastern Mediterranean: Identification and definition. *Theor. Appl. Climatol.* **71**: 17–28, doi: 10.1007/s704-002-8205-x.

Kutiel H, Helfman I. 2004. The impact of Central African-Caspian Oscillation (Caco) on climate regimes in the Red Sea region. *Horizons Geogr.* **60–61**: 183–194.

Kutiel H, Kay PA. 1992. Recent variations in 700 hPa geopotential heights in summer over Europe and the Middle East, and their influence on other Meteorological factors. *Theor. Appl. Climatol.* **46**: 99–108, doi: 10.1007/bf00866089.

Kutiel H, Türkeş M. 2005. New evidence for the role of the North Sea – Caspian pattern on the temperature and precipitation regimes in continental central Turkey. *Geogr. Ann.* **87 A**: 501–513.

Kutiel H, Maheras P, Türkeş M, Paz S. 2002. North Sea – Caspian Pattern (*NCP*) – an upper level atmospheric teleconnection affecting the eastern Mediterranean – implications on the regional climate. *Theor. Appl. Climatol.* **72**: 173–192, doi: 10.1007/s00704-002-0674-8.

Lee D, Biasutti M. 2014. Climatology and variability of precipitation in the twentieth-century reanalysis. *J. Clim.* **27**: 5964–5981, doi: 10.1175/JCLI-D-13-00630.1.

Li L, Bozec A, Somot S, Béranger K, Bouruet-Aubertot P, Sevault F, Crépon M. 2006. Chapter 7 Regional atmospheric, marine processes and climate modelling. In *Mediterranean Climate Variability*, Lionello P, Malanotte-Rizzoli P, Boscolo R (eds). Elsevier: Amsterdam.

Lionello P, Malanotte-Rizzoli P, Boscolo R, Alpert P, Artale V, Li L, Luterbacher J, May W, Trigo R, Tsimplis M, Ulbrich U, Xoplaki E.

2006. The Mediterranean climate: an overview of the main characteristics and issues. In *Mediterranean Climate Variability*, Lionello P, Malanotte-Rizzoli P, Boscolo R (eds). Elsevier: Amsterdam.

Llopart M, Coppola E, Giorgi F, da Rocha RP, Cuadra SV. 2014. Climate change impact on precipitation for the Amazon and La Plata basins. *Clim. Change* **125**: 111, doi: 10.1007/s10584-014-1140-1.

Martin-Vide J, Lopez-Bustins J-A. 2006. The Western Mediterranean Oscillation and rainfall in the Iberian Peninsula. *Int. J. Climatol.* **26**: 1455–1475, doi: 10.1002/joc.1388.

McIlveen R. 2010. *Fundamentals of Weather and Climate*, 2nd edn. Oxford University Press: New York, NY.

Meehl GA, van Loon H. 1979. The seesaw in winter temperatures between Greenland and Northern Europe. Part III: teleconnections with lower latitudes. *Mon. Weather Rev.* **107**: 1095–1106, doi: 10.1175/1520-0493(1979)107<1095:tsiwtb>2.0.co;2.

Moore GWK, Renfrew IA, Pickart RS. 2013. Multidecadal mobility of the North Atlantic Oscillation. *J. Clim.* **26**: 2453–2466.

Moulin C, Lambert CE, Dulac F, Dayan U. 1997. Control of atmospheric export of dust from North Africa by the North Atlantic Oscillation. *Nature* **387**: 691–694.

Murphy J. 1999. An evaluation of statistical and dynamical techniques for downscaling local climate. *J. Clim.* **12**: 2256–2284.

Ozturk T, Altinsoy HA, Türkes M, Kurnaz ML. 2012. Simulation of temperature and precipitation climatology for the Central Asia CORDEX domain using RegCM 4.0. *Clim. Res.* **52**: 63–76, doi: 10.3354/cr01082.

Palutikof J. 2003. Analysis of Mediterranean climate data: measured and modelled. In *Mediterranean Climate: Variability and Trends*, Bolle HJ (ed). Springer-Verlag: Berlin.

Palutikof JP, Conte M, Casimiro Mendes J, Goodess CM, Espirito Santo F. 1996. Climate and climatic change. In *Mediterranean Desertification and Land Use*, Brandt CJ, Thornes JB (eds). John Wiley & Sons: London.

Paz S, Tourre YM, Planton S. 2003. North Africa-West Asia (NAWA) sea-level pressure patterns and their linkages with the Eastern Mediterranean (EM) climate. *Geophys. Res. Lett.* **30**: 1999, doi: 10.1029/2003GL017862.

Reboita MS, Fernandez JPR, Pereira Llopart M, Porfirio da Rocha R, Albertani Pampuch L, Cruz FT. 2014. Assessment of RegCM4.3 over the CORDEX South America domain: sensitivity analysis for physical parameterization schemes. *Clim. Res.* **60**: 215–234, doi: 10.3354/cr01239.

Roeckner E, Bäuml G, Bonaventura L, Brokopf R, Esch M, Giorgetta M, Hagemann S, Kirchner I, Kornblueh L, Manzini E, Rhodin A, Schlese U, Schulzweida U, Tompkins A. 2003. The atmospheric general circulation model ECHAM5. I. model description. Report No. 349, Max-Planck Institute for Meteorology, Hamburg, Germany.

Roeckner E, Brokopf R, Esch M, Giorgetta M, Hagemann S, Kornblueh L, Manzini E, Schlese U, Schulzweida U. 2006. Sensitivity of simulated climate to horizontal and vertical resolution in the ECHAM5 atmosphere model. *J. Clim.* **19**: 3771–3791, doi: 10.1175/JCLI3824.1.

Rogers JC. 1990. Patterns of low-frequency monthly sea level pressure variability (1899–1986) and associated wave cyclone frequencies. *J. Clim.* **3**: 1364–1379, doi: 10.1175/1520-0442(1990)003<1364:polfms>2.0.co;2.

Thompson DWJ, Wallace JM. 1998. The Arctic oscillation signature in the wintertime geopotential height and temperature fields. *Geophys. Res. Lett.* **25**: 1297–1300, doi: 10.1029/98GL00950.

Tourre YM, Paz S. 2004. The North-Africa/Western Asia (NAWA) sea level pressure index: a Mediterranean signature of the Northern Annular Mode (NAM). *Geophys. Res. Lett.* **31**: L17209, doi: 10.1029/2004GL020414.

Tourre YM, Paz S, Cassou C, Kutiel H. 2006. Atmospheric dynamics over northwest Africa and linkages with Sahelian rainfall. *Geophys. Res. Lett.* **33**: L14808, doi: 10.1029/2006GL026695.

Trigo RM, Palutikof JP. 2001. Precipitation scenarios over Iberia: a comparison between direct GCM output and different downscaling techniques. *J. Clim.* **14**: 4422–4446, doi: 10.1175/1520-0442(2001)014<4422:PSOIAC>2.0.CO;2.

Trigo RM, Osborn TJ, Corte-Real JM. 2002. The North Atlantic Oscillation influence on Europe: climate impacts and associated physical mechanisms. *Climate Res.* **20**: 9–17.

Trigo RM, Pozo-Vázquez D, Osborn TJ, Castro-Díez Y, Gámiz-Fortis S, Esteban-Parra MJ. 2004. North Atlantic Oscillation influence on precipitation, river flow and water resources in the Iberian Peninsula. *Int. J. Climatol.* **24**: 925–944.

Vicente-Serrano SM, Begueria S, López-Moreno JI, Kenawy AME, Angulo-Martínez M. 2009. Daily atmospheric circulation events and extreme precipitation risk in northeast Spain: Role of the North Atlantic Oscillation, the Western Mediterranean Oscillation, and the Mediterranean Oscillation. *J. Geophys. Res.* **114**: D08106, doi: 10.1029/2008JD011492.

Vinther BM, Andersen KK, Hansen AW, Schmith T, Jones PD. 2003. Improving the Gibraltar/Reykjavik NAO index. *Geophys. Res. Lett.* **30**: 2222.

Walker GT, Bliss EW. 1934. World weather V. *Mem. Roy. Meteor. Soc.* **IV**: 53–84.

Wallace JM, Gutzler DS. 1981. Teleconnections in the geopotential height field during the Northern Hemisphere winter. *Mon. Weather Rev.* **109**: 784–812, doi: 10.1175/1520-0493(1981)109<0784:TITGHF>2.0.CO;2.

Whitaker JS, Compo GP, Wei X, Hamill TM. 2004. Reanalysis without radiosondes using ensemble data assimilation. *Mon. Weather Rev.* **132**: 1190–1200.

Zorita E, vonStorch H. 1999. The analog method as a simple statistical downscaling technique: comparison with more complicated methods. *J. Clim.* **12**: 2474–2489.

